

A Fast Algorithm for GVF Snake Model

TANG Ke-lun¹, TANG Yong-liang¹, ZENG Wei², JIA Hai-yang¹, ZHANG Yang¹, LIU Yan¹

(1. School of Mechanical Engineering, Sichuan University of Science and Engineering, Zigong 64300, Sichuan, China;

2. Zigong K/D CARBON CO., LTD, 643000, Sichuan, China)

Abstract: A research on difference scheme of image gravitational field in the GVF snake model is performed depending on the uniform stability and convergence conditions of the difference scheme. It is found that the original explicit forward difference scheme puts a strict restriction on the diffusion coefficient in the partial differential equation which decelerates the convergence speed of difference equation iteration. A new difference scheme is put forward, which has the advantage of unconditional uniform stability and convergence, and the restriction on the coefficient of partial differential equation is removed. Through increasing the value of the coefficient appropriately, the image of boundary information transmission becomes faster. Hence, iteration calculations are decreased rapidly for a given transmission range. The simulation experiments indicate that the new difference scheme be higher efficiency than the traditional one.

Keywords: GVF Snake Model; Image Gravitational Field; Difference Scheme

中图分类号:TP751.1

文献标志码:A

1 INTRODUCTION

Active contour model (snake model) was proposed in 1987 and was succeeded in tracing the mouth movement on face by Kass^[1]. Snake is an energy - minimizing curve. Its shape is constrained by internal forces, and it was dragged to significant image characters by image force. The algorithm is equal to a constrained optimization method, and the inner constraint energy can be defined according to the specific shape of the object, which gives the model more flexible and gives a uniform solution for a wide range of visual problems. Therefore, the algorithm has been successfully applied in many areas of Computer Vision by more and more researchers, such as edge extraction^[2], object reconstruc-

tion^[3,4], motion track^[3], image segmentation and classification^[5], stereo matching etc^[6]. However, there are many deficiencies in the snake model, such as sensitive to the initial contour position and noise, poor convergence to the concave contours.

According to many disadvantages of the traditional snake model, many efforts have been made to improve this model^[7]. Xu and Prince^[8] proposed the gradient vector flow (GVF) snake model in 1997. It enlarges the capture range of traditional active contour model, and can guides the contours tracing into the concavities of the object boundary. In this model, a force field $V(x, y) = [u(x, y), v(x, y)]$ is defined from the image by minimizing the energy function:

$$E = \iint \mu(u_x^2 + u_y^2 + v_x^2 + v_y^2) + |\nabla f|^2 |V - \nabla f|^2 dx dy \quad (1)$$

收稿日期:2012-12-01

基金项目:国家“十一五”科技支撑计划项目(2008BADC4B15);四川省教育厅科研项目(10ZB097);四川理工学院人才引进项目(2009XJKRL002);过程装备与控制工程四川省高校重点实验室项目(GKYJ201101, GK200907)

作者简介:唐克伦(1972-),男,四川泸县人,教授,博士,主要从事计算机图像处理、计算力学等方面的研究,(E-mail)cagd@tom.com

Where, $f = |\nabla I(x, y)|^2$, μ is the diffusion coefficient which regulates the weights of the first and the second item (the more image noise, and the greater μ) and plays an important role in the diffusion velocity of the image contour in smooth region away from the contour. In this equation, near the object boundary, $|\nabla f|$ is large, the second term dominates and the minimization gives $V = \nabla f$; while away from the object boundary, $|\nabla f|$ is small and thus the second term is small, the energy is dominated by the diffusion term, which means the force V is extended smoothly from its value near the object boundary^[9]. Therefore, the capture range is larger than classic active contour model and there is no need to place the initial curve entirely inside or outside the object contours.

The force field V is obtained through solving the partial differential equation of image gravitational field, so the difference scheme has an important influence on the efficiency and accuracy of the force field. In order to prevent the divergent result being triggered by the magnifying discretization error of initial condition in the interactive process, there are restrictions on the uniform stability and convergence conditions in the original explicit forward difference scheme, which restrict the step size of the discrete grids and the value of diffusion coefficient μ , hence reduce the computational efficiency for image gravitational field in the GVF snake model, especially the high-definition image with much noise.

In order to improve the computational efficiency for image gravitational field in the GVF snake model, a new difference scheme is proposed, which has advantages of unconditional consistent stability and convergence, increases flexibility about parameters' selection of discrete grids, and finds good trade-off between accuracy and velocity of the calculation. The simulation results show that calculation speed of image gravitational field in the GVF snake model can be improved rapidly by the new difference scheme through increasing the value of diffusion coefficient μ . Furthermore, an optimized value for diffusion coefficient μ is also discussed.

2 EXPLICIT DIFFERENCE SCHEME

The GVF snake model differs from traditional snake model in the external energy function. The corresponding

evolution equations of the minimized energy function (1) can be obtained by gradient descent algorithm as follows^[11]:

$$\begin{cases} \frac{\partial u}{\partial t} = \mu \left(\frac{\partial^2 u}{\partial x^2} + \frac{\partial^2 u}{\partial y^2} \right) - (u - f_x)(f_x^2 + f_y^2) \\ \frac{\partial v}{\partial t} = \mu \left(\frac{\partial^2 v}{\partial x^2} + \frac{\partial^2 v}{\partial y^2} \right) - (v - f_y)(f_x^2 + f_y^2) \end{cases} \quad (2)$$

Satisfying the following boundary conditions:

$$\begin{cases} (u(x, y, 0) = f_x(x, y), (x, y) \in \Omega \\ (v(x, y, 0) = f_y(x, y), (x, y) \in \Omega \end{cases} \quad (3)$$

Where, $f_x = df(x, y)/dx$, $f_y = df(x, y)/dy$. The definite solution of partial differential equations (2) in the initial-boundary value problem can be solved by the Finite Difference method. In order to establish a difference scheme, let

$$\begin{cases} b(x, y) = f_x^2(x, y) + f_y^2(x, y) \\ c^1(x, y) = f_x(x, y)b(x, y) \\ c^2(x, y) = f_y(x, y)b(x, y) \end{cases} \quad (4)$$

Simultaneously, considering the forward difference in time and the centered difference in space:

$$\begin{cases} \frac{\partial u}{\partial t} \approx \frac{u_{i,j}^{n+1} - u_{i,j}^n}{\tau} \\ \frac{\partial v}{\partial t} \approx \frac{v_{i,j}^{n+1} - v_{i,j}^n}{\tau} \\ \frac{\partial^2 u}{\partial x^2} \approx \frac{u_{i+1,j}^n + u_{i-1,j}^n - 2u_{i,j}^n}{h_x^2} \\ \frac{\partial^2 u}{\partial y^2} \approx \frac{u_{i,j+1}^n + u_{i,j-1}^n - 2u_{i,j}^n}{h_y^2} \\ \frac{\partial^2 v}{\partial x^2} \approx \frac{v_{i+1,j}^n + v_{i-1,j}^n - 2v_{i,j}^n}{h_x^2} \\ \frac{\partial^2 v}{\partial y^2} \approx \frac{v_{i,j+1}^n + v_{i,j-1}^n - 2v_{i,j}^n}{h_y^2} \end{cases} \quad (5)$$

Where, h_x , h_y and τ are corresponding mesh steps. Let $h_x = h_y = h$, substitute Eq. (4) and Eq. (5) into Eq. (2), the explicit forward difference scheme of the image gravitational field in the GVF snake model is^[8].

$$\begin{cases} u_{i,j}^{n+1} = (1 - b_{i,j}\tau - 4r)u_{i,j}^n + c_{i,j}^1\tau + r(u_{i+1,j}^n + u_{i-1,j}^n + u_{i,j+1}^n + u_{i,j-1}^n) \\ v_{i,j}^{n+1} = (1 - b_{i,j}\tau - 4r)v_{i,j}^n + c_{i,j}^2\tau + r(v_{i+1,j}^n + v_{i-1,j}^n + v_{i,j+1}^n + v_{i,j-1}^n) \end{cases} \quad (6)$$

Where, $r = \mu\tau/h^2$. According to the discrete maximum principle of Difference Equations Solution, if $b(x, y)$, $c^1(x,$

$\gamma), c^2(x, y)$ have bounded initial values, the uniform stability and convergence condition of the explicit forward difference scheme is^[8]

$$r = \mu\tau/h^2 \leq 0.25 \quad (7)$$

or

$$\mu \leq h^2/4\tau \quad (8)$$

From Eq. (8), the diffusion coefficient μ is restricted not to exceed a specified value; otherwise, the result of image gravitational field in the GVF snake model will be divergent. Correspondingly, the mesh step h in a digital image is ordinarily assumed as 1 pixel, and the mesh step is assumed as an iterative step size. Therefore, $h = 1, \tau = 1$ and the uniform stability and convergence condition of difference scheme is^[12].

$$\mu \leq 0.25 \quad (9)$$

From the Eq. (9), the value of diffusion coefficient μ is constraint in a small range in order to satisfy the uniform stability and convergence condition of difference scheme. Experiments indicate higher value of the diffusion coefficient μ would help the boundary information to transmit faster. A tradeoff numerical value of the diffusion coefficient μ between the stability and the boundary information transmission speed is about 0.2.

In order to break through the constraint on the value of diffusion coefficient μ so that a higher boundary information transmission speed is obtained, and a new difference scheme is promoted.

3 IMPLICIT DIFFERENCE SCHEME

3.1 Establishment of Implicit Difference Scheme

Choose the backward difference in time and the centered difference in space, yield

$$\begin{cases} \frac{\partial u}{\partial t} \approx \frac{u_{i,j}^{n+1} - u_{i,j}^n}{\tau} \\ \frac{\partial v}{\partial t} \approx \frac{v_{i,j}^{n+1} - v_{i,j}^n}{\tau} \\ \frac{\partial^2 u}{\partial x^2} \approx \frac{u_{i+1,j}^{n+1} + u_{i-1,j}^{n+1} - 2u_{i,j}^{n+1}}{h_x^2} \\ \frac{\partial^2 u}{\partial y^2} \approx \frac{u_{i,j+1}^{n+1} + u_{i,j-1}^{n+1} - 2u_{i,j}^{n+1}}{h_y^2} \\ \frac{\partial^2 v}{\partial x^2} \approx \frac{v_{i+1,j}^{n+1} + v_{i-1,j}^{n+1} - 2v_{i,j}^{n+1}}{h_x^2} \\ \frac{\partial^2 v}{\partial y^2} \approx \frac{v_{i,j+1}^{n+1} + v_{i,j-1}^{n+1} - 2v_{i,j}^{n+1}}{h_y^2} \end{cases} \quad (10)$$

Let $h_x = h_y = h$, substitute Eq. (10) and Eq. (4) into Eq. (2), the iterative scheme of the explicit backward difference of the image gravitational field in the GVF snake model

$$\begin{cases} (1 + b_{i,j}\tau + 4r)u_{i,j}^{n+1} - r(u_{i+1,j}^{n+1} + u_{i-1,j}^{n+1} + u_{i,j+1}^{n+1} + u_{i,j-1}^{n+1}) = u_{i,j}^n + c_{i,j}^1\tau \\ (1 + b_{i,j}\tau + 4r)v_{i,j}^{n+1} - r(v_{i+1,j}^{n+1} + v_{i-1,j}^{n+1} + v_{i,j+1}^{n+1} + v_{i,j-1}^{n+1}) = v_{i,j}^n + c_{i,j}^2\tau \end{cases} \quad (11)$$

Define

$$\begin{aligned} u &= (u_{1,1}, u_{2,1}, \dots, u_{M,1}, u_{1,2}, u_{2,2}, \dots, u_{M,2}, \dots, \\ &\quad u_{1,N}, u_{2,N}, \dots, u_{M,N})^T \\ v &= (v_{1,1}, v_{2,1}, \dots, v_{M,1}, v_{1,2}, v_{2,2}, \dots, v_{M,2}, \dots, \\ &\quad v_{1,N}, v_{2,N}, \dots, v_{M,N})^T \\ b &= (b_{1,1}, b_{2,1}, \dots, b_{M,1}, b_{1,2}, b_{2,2}, \dots, b_{M,2}, \dots, \\ &\quad b_{1,N}, b_{2,N}, \dots, b_{M,N})^T \\ c^1 &= (c_{1,1}^1, c_{2,1}^1, \dots, c_{M,1}^1, c_{1,2}^1, c_{2,2}^1, \dots, c_{M,2}^1, \dots, \\ &\quad c_{1,N}^1, c_{2,N}^1, \dots, c_{M,N}^1)^T \\ c^2 &= (c_{1,1}^2, c_{2,1}^2, \dots, c_{M,1}^2, c_{1,2}^2, c_{2,2}^2, \dots, c_{M,2}^2, \dots, \\ &\quad c_{1,N}^2, c_{2,N}^2, \dots, c_{M,N}^2)^T \end{aligned}$$

Where, M, N is the number of grid in the directions of x and y . The grid nodes are of non-natural order which is from left to right ($i \uparrow$), from down to up ($j \uparrow$). So Eq. (9) can be transferred to equivalent linear equations:

$$\begin{cases} Au^{n+1} = f_u^n \\ Av^{n+1} = f_v^n \end{cases} \quad (12)$$

Where

$$A = \begin{pmatrix} B_1 & -E & & & & \\ -E & B_2 & -E & & & \\ & -E & B_3 & -E & & \\ & & \ddots & \ddots & \ddots & \\ & & & -E & B_{N-1} & -E \\ & & & & -E & B_N \end{pmatrix}$$

Where E is a unit matrix of M -order, B_i are tri-diagonal sub matrices of M -order

$$B_i = \begin{pmatrix} e_{i,1} & -1 & & & & \\ -1 & e_{i,2} & -1 & & & \\ & -1 & e_{i,3} & -1 & & \\ & & \ddots & \ddots & \ddots & \\ & & & -1 & e_{i,M-1} & -1 \\ & & & & -1 & e_{i,M} \end{pmatrix}$$

and $e_{i,j} = 4 + (1 + b_{i,j}\tau)/r$,

$$f_u^n = (u^n + c^1\tau)/r, f_v^n = (v^n + c^2\tau)/r.$$

3.2 Fourier – von Neumann Stability Analysis

The stability of finite difference schemes is closely associated with numerical errors. A finite difference scheme is stable if the errors made at one time step of the calculation do not cause the errors to increase as the computations are continued. So the uniform stability of implicit difference Eq. (9) is determined by the error $\mathcal{E}_{j,k}^0$ which is introduced during the discretion of the initial condition, not being amplified during the calculation of the difference scheme (the discretion of the boundary condition and the solving process of the difference equation are assumed not to introduce any other errors).

Define the numerical error $\mathcal{E}_{j,k}^n$ as

$$\mathcal{E}_{j,k}^n = \widetilde{u}_{j,k}^n - u_{j,k}^n \tag{13}$$

where, $\widetilde{u}_{j,k}^n$ is the numerical solution obtained in finite precision arithmetic, $u_{j,k}^n$ is the solution of implicit difference Eq. (11). Since the exact solution $u_{j,k}^n$ must satisfy the discretized equation exactly, the error $\mathcal{E}_{j,k}^n$ must also satisfy the discretized equation^[13].

$$\begin{cases} (I + b\tau - r\delta_y^2)\mathcal{E}_{j,k}^{n+1} = \mathcal{E}_{j,k}^n \\ (j,k) \in \Omega_h, 0 \leq n < N \\ \mathcal{E}_{j,k}^0 = c \quad (j,k) \in \Omega_h \\ \mathcal{E}_{j,k}^0 = 0 \quad (j,k) \in \partial\Omega_h \end{cases} \tag{14}$$

where, δ_x^2, δ_y^2 is the finite difference operator, and c is a constant. The Eq. (11) and Eq. (14) shows that both the error $\mathcal{E}_{j,k}^n$ and the numerical solution $u_{j,k}^n$ have the same growth or decay behavior with respect to time. For linear differential equations with periodic boundary condition, the spatial variation of error $\mathcal{E}_{j,k}^n$ may be expanded in a two – dimensional Fourier series.

$$\begin{aligned} \mathcal{E}^{n+1}(x,y) &= \sum_{l_x, l_y = -\infty}^{+\infty} \xi_{l_x, l_y}^{n+1} e^{i2\pi(l_x x + l_y y)} \\ &= \sum_{l_x, l_y = -\infty}^{+\infty} \xi_{l_x, l_y}^{n+1} e^{i(\beta_x x + \beta_y y)} \end{aligned} \tag{15}$$

Where, $\beta_x = 2\pi l_x, \beta_y = 2\pi l_y, \xi_{l_x, l_y}^{n+1}$ satisfy Parseval equality^[16].

$$\int_0^1 \int_0^1 |\mathcal{E}^{n+1}(x,y)|^2 dx dy = \sum_{l_x, l_y = -\infty}^{+\infty} |\xi_{l_x, l_y}^{n+1}|^2 \tag{16}$$

Since the difference equation for error is linear (the behavior of each term of the series is the same as series itself), it is enough to consider the growth of error of a typi-

cal term

$$\mathcal{E}_{j,k}^{n+1} = \xi_{l_x, l_y}^{n+1} e^{i(\beta_x h_x + \beta_y h_y)} \tag{17}$$

By substitute Eq. (17) into discretized Eq. (14), we obtain^[14, 16]

$$\begin{aligned} (I + b\tau + 4r\sin^2(\beta_x h_x/2) + \\ 4r\sin^2(\beta_y h_y/2)) \xi_{l_x, l_y}^{n+1} = \xi_{l_x, l_y}^n \end{aligned} \tag{18}$$

Define the amplification factor

$$G(\beta_x, \beta_y, \tau) = \xi_{l_x, l_y}^{n+1} / \xi_{l_x, l_y}^n \tag{19}$$

So the amplification factor of the implicit difference Eq. (11) is

$$\begin{aligned} G(\beta_x, \beta_y, \tau) = (I + b\tau + 4r\sin^2(\beta_x h_x/2) + \\ 4r\sin^2(\beta_y h_y/2))^{-1} \end{aligned} \tag{20}$$

For $b = |\nabla f|^2$, obviously, the formula is tenable for any β_x, β_y , and r as follows:

$$|G(\beta_x, \beta_y, \tau)| \leq 1 \tag{21}$$

Therefore, according to Lax Equivalence Theorem^[15], the implicit difference Eq. (11) is unconditional uniform stability and convergence. Consequently, the value of diffusion coefficient μ is of no limits and larger value can be obtained. Through appropriately increasing the value of diffusion coefficient μ , the diffusion speed of the image contour is significantly improved, and less iteration is needed.

4 THE ALGORITHM IMPLEMENTATION AND NUMERICAL EXPERIMENT

4.1 The Algorithm Implementation

Although the new difference scheme set no limits to μ and the diffusion speed of the image contour can be significantly improved through appropriately increasing the value of μ , the algorithm implementation is more complex than that in the traditional explicit forward difference scheme due to the large sparse three – diagonal square – matrix implicit Eq. (12). The highly efficient formation of matrix A and the proper solution method have a direct relation to the solution efficiency and accuracy. Matrix A is a diagonally – dominant matrix, and the diagonal elements of fluctuation range ($e_{i,j} = 4 + (1 + b_{i,j}\tau)/r, 0 \leq b_{i,j} = |\nabla f_{i,j}|^2 \leq \sqrt{2}$) are small. Therefore, the condition number A of coefficient matrix A is reasonable, and the steepest descent method without preprocess can be used.

The algorithm is designed as follows

Algorithm: Unpreconditioned Steepest Descent Iteration

```

1  [f, μ, n] ← get_initialization_imgf(image)
2   $f_x \leftarrow \frac{df}{dx}; f_y \leftarrow \frac{df}{dy}; b = (f_x^2 + f_y^2 + 1)/\mu$ 
3  [ms, ns] ← size(f)
% returns the size of matrix f in separate variables m and n
4  P ← zeros(ns, ns); Q ← zeros(ms, ms)
5  P(i+1,i)} ← -1 (i = 1, 2, 3, ..., ns)
   Q(j+1,j)} ← -1 (j = 1, 2, 3, ..., ms)
6  P ← P + PT; Q ← Q + QT + 4Ems
7  A ← P ⊗ Ems + Ens ⊗ Q
% represents the Kronecker product of the two matrix
8  A ← A + diag(b1,1, b2,1, ..., bms,1, b1,2, b2,2, ..., bms,2, ..., b1,m,
   b2,m, ..., bms,m)
9  c1 ← vec[fxO(fx2 + fy2)/μ]
% Orepresents the Hadamard product of the two matrix
10 c2 ← vec[fyO(fx2 + fy2)/μ]
11 Iterate = 1, 2, ... until n
12  bx ← c1 + u/μ
13  Initialize : r0 ← bx - Au0
14  Iterate k = 0, 1, ... until convergence
15   $\partial^k \leftarrow \langle r^k, r^k \rangle / \langle r^k, Ar^k \rangle$ 
16  uk+1 ← uk + ∂krk
17  rk+1 ← rk + ∂kArk
18  end
19  by ← c2 + v/μ
20  Initialize : r0 ← by - Av0
21  Iterate k = 0, 1, ... until convergence
22   $\partial^k \leftarrow \langle r^k, r^k \rangle / \langle r^k, Ar^k \rangle$ 
23  vk+1 ← vk + ∂krk
24  rk+1 ← rk - ∂kArk
25  end
26  end
27  [u, v] ← vec_to_matrix(u, v)
% vector to matrix

```

4.2 The Numerical Experiment

The computer simulation experiment was performed in the following software and hardware environments. Computer type: HP ProLiant DL585 G7 Rack Mount Chassis; Operating System: Windows 7 Server Standard (64 bit); Simulation Software: MATLAB 2011 b (64 bit); CPU: 4AMD Opteron 6136; Memory: 64GB DDR3 DIMMs PC2 - 6400 DDR SDRAM.

Fig. 1 shows the gradient vector flow field for a window - like picture (64 × 64 pixels). The diffusion coefficient μ from Fig. 1 (a) - (d) are 0.2, 0.5, 1 and 2 respectively, and T represents the calculation time consuming. Their iteration numbers are all set to 10. Fig. 1 (a) is performed through the traditional explicit difference scheme, and Fig. 1 (b) - (d) are performed through the implicit difference scheme. Fig. 1 shows

that calculation speed of the traditional explicit difference scheme is slightly faster than that of the implicit difference scheme. However, its image contour information diffusion range is obviously smaller under the same iterations.

For further comparisons, pictures with different sizes are adopted. Table 1 - 4 exhibits comparisons in the time consuming (T) and the speed up ratio (S_p) under almost the same diffusion range. From Table 1, the computation of the explicit difference scheme with $\mu = 0.1$ will need 150 iterations, while the computation of the implicit difference scheme with $\mu = 0.50$ will only need 30 iterations; $S_p = 5.4252$ with 100×100 pixels gradually increases to $S_p = 11.2910$ with 3200×3200 pixels, which implies that the speed up ratio is more evident for the large - size pictures. The performance of implicit difference scheme through increase the value of μ is significant. From Table 1 - 2, when $\mu \leq 1$, the speed up ratio is almost proportional to the value of μ , From Table 2 - 4, when $\mu > 1$, the increasing of convergence speed begins not evidently. In order to obtain an optimized value of μ , the chart of the speed up ratio (S_p) is drawn. From Fig. 2, the speed up ratio (S_p) is almost no change with the increasing of μ when $\mu \geq 2$. Therefore, the optimal value of the diffusion coefficient μ is about 2.

Table 1 Performance comparison between explicit difference scheme ($\mu = 0.10$) and implicit difference scheme ($\mu = 0.50$)

experimental picture (pixel)	explicit difference scheme ($\mu = 0.10$)		implicit difference scheme ($\mu = 0.50$)		$S_p(T/T_{0.50})$
	n	$T(s)$	$N_{0.50}$	$T_{0.50}(s)$	
100 × 100	150	0.4823	30	0.0889	5.4252
200 × 200	150	5.9860	30	0.9843	6.0815
400 × 400	150	50.2336	30	7.9578	6.3125
800 × 800	150	283.585	30	27.3314	10.375
1600 × 1600	150	774.483	30	70.7150	11.192
3200 × 3200	150	3138.10	30	281.321	11.291

Table 2 Performance comparison between explicit difference scheme ($\mu = 0.10$) and implicit difference scheme ($\mu = 1.00$)

experimental picture (pixel)	explicit difference scheme ($\mu = 0.10$)		implicit difference scheme ($\mu = 1.00$)		$S_p(T/T_{1.00})$
	n	$T(s)$	$n_{1.00}$	$T_{1.00}(s)$	
100 × 100	150	0.4823	16	0.0514	9.3833
200 × 200	150	5.9860	16	0.5929	10.0961
400 × 400	150	50.2336	16	4.5055	11.1494
800 × 800	150	283.585	16	15.0820	18.8029
1600 × 1600	150	774.483	16	41.7150	18.9736
3200 × 3200	150	3138.10	16	166.8924	19.1672

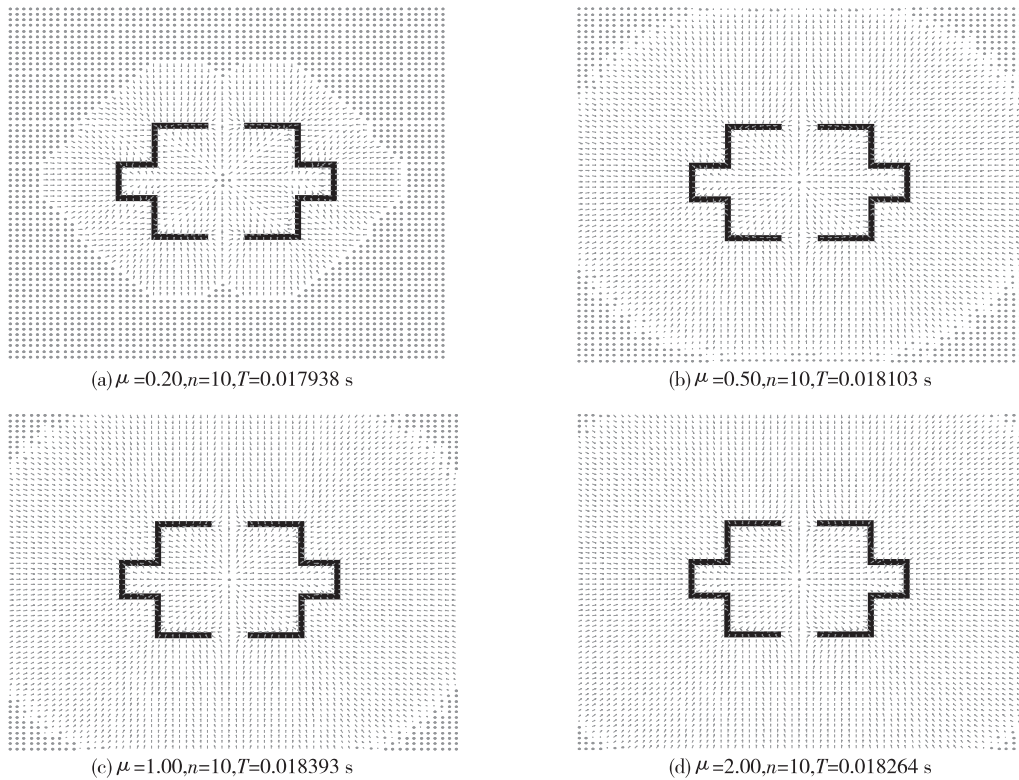


Fig. 1 the gradient vector flow field for a window – like picture

Table 3 Performance comparison between explicit difference scheme ($\mu = 0.10$) and implicit difference scheme ($\mu = 2.00$)

experimental picture (pixel)	explicit difference scheme ($\mu = 0.10$)		implicit difference scheme ($\mu = 2.00$)		$S_p (T / T_{2.00})$
	n	$T(s)$	$N_{2.00}$	$T_{2.00}(s)$	
100 × 100	150	0.4823	13	0.0436	11.0619
200 × 200	150	5.9860	13	0.4977	12.0273
400 × 400	150	50.2336	13	3.7485	13.4010
800 × 800	150	283.585	13	13.0806	21.6791
1600 × 1600	150	774.483	13	34.3201	23.0619
3200 × 3200	150	3138.10	13	132.5911	23.6675

Table 4 Performance comparison between explicit difference scheme ($\mu = 0.10$) and implicit difference scheme ($\mu = 5.0$)

experimental picture (pixel)	explicit difference scheme ($\mu = 0.10$)		implicit difference scheme ($\mu = 5.00$)		$S_p (T / T_{5.00})$
	n	$T(s)$	$N_{5.00}$	$T_{5.00}(s)$	
100 × 100	150	0.4823	12	0.0406	11.8793
200 × 200	150	5.9860	12	0.4274	14.0056
400 × 400	150	50.2336	12	3.4709	14.4728
800 × 800	150	283.585	12	12.1680	23.3058
1600 × 1600	150	774.483	12	33.4781	23.6419
3200 × 3200	150	3138.10	12	129.9449	24.7204

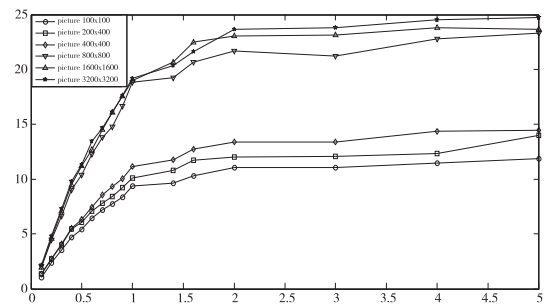


Fig. 2 The relationship between the speed up ratio S_p and the diffusion coefficient μ

5 CONCLUSIONS

In order to improve the contour extraction speed, the external force field of image in the active contour models; the gradient vector flow is researched. An implicit difference scheme is proposed which break through the value constraints of the diffusion coefficient μ . Compared with the traditional explicit difference scheme, larger value of the diffusion coefficient μ can be set in this implicit difference scheme. Through increasing the value of μ appropriately, faster diffusion speed can be achieved. The numerical experiment results indicated that the time consuming in this

implicit difference scheme will be shortened to less than 10% , and the optimal value of the diffusion coefficient μ is about 2. Consequently, it is more suitable to be applied to real - time image processing applications.

ACKNOWLEDGMENTS

MATLAB snake demo toolbox developed by Xu C. and Prince J. is used in this paper, which helps the author to learn active contour models. This work is supported by the National Key Technology R&D Program for the 11th five-year plan (NO. 2008BAD4B15) , Dr. Start Fund Project of Sichuan University of Science and Engineering (NO. 2010ZY019) , the project of youth fund of Sichuan Province (NO. 10ZB097) , the project for talent introduction of Sichuan University of Science and Engineering (NO. 2009XJKL002) and the Graduate Student Innovation Fund of Sichuan University of Science and Engineering (NO. Y2011001) .

References:

- [1] Kass M, Witkin A, Terzopoulos D. Snake, Active contour model[J]. International Journal of Computer Vision, 1987, (1):321-331.
- [2] Jolly MP. Automatic segmentation of the left ventricle in cardiac MR and CT images[J]. International Journal of Computer Vision, 2006, 70(2):151-163.
- [3] Terzopoulos D, Fleischer K. Deformable models[J]. The Visual Computer, 1988, 4(1):306-331.
- [4] McInerney T, Terzopoulos D. A dynamic finite element surface model for segmentation and tracking in multidimensional medical images with application to cardiac 4D image analysis [J]. Computerized Medical Imaging and Graphics, 1995, 19(1):69-83.
- [5] Leymarie F, Levine M D. Tracking deformable objects in the plane using an active contour model[J]. IEEE Trans. On Pattern Anal. Machine Intell, 1993, 15(6):617-634.
- [6] Chen Zonghai, Fang Wei1, Chen Huiyong, et al. Active contour model based on distribution matching and its image segmentation algorithm[J]. Journal of Jilin University (Engineering and Technology Edition), 2008, 38 (6): 1441-1446.
- [7] Wang Wenzhe, Tang Kelun, Mou Zongkui, et al. Segmented B-snake Model[J]. Journal of Sichuan University of Science & Engineering (Natural Science Edition), 2009, 22(5), 096-0100.
- [8] Xu C, Prince J L. Gradient vector flow: a new external force for snake[J]. Comp. Vis. Patt. Recog. (CVPR), 1997, 2(3):66-71.
- [9] Yang Xiang, Albert C S, Chung Jianye. An active contour model for image segmentation based on elastic interaction[J]. Journal of Computational Physics, 2006, 219:455-476.
- [10] Ning Jifeng, Wu Chengke, Liu Shigang, et al. NGVF: an improved external force field for active contour model [J]. Pattern Recognition Letters, 2007, 28:58-63.
- [11] Tang Kelun, Zhang Xiangwei, Cheng Siyuan. Improved GVF snake[C]. International conference on sense, computing and automation 2006 (ICSCA'2006). 2006: 162-165.
- [12] Tang Kelun, Zhang Xiangwei, Cheng Siyuan. Inertia force, pressure force and GVF for active contour[J]. Journal of information and computational science, 2006, 3 (2): 287-294.
- [13] Anderson John David Jr. Computational fluid dynamics: the basics with applications[M]. New York: McGraw Hill, 1994.
- [14] Richard Haberman. Applied partial differential equations: with fourier series and boundary value problems[M]. 4th ed. San Francisco: Pearson Education, Inc. 2004.
- [15] Lax P, Richtmyer R D. Survey of the stability of linear finite difference equations[J]. Comm. Pure Appl. Math, 1956, 9:267-293.
- [16] Yu Dehao, Tang huazhong. Numerical solution of differential equation[M]. Beijing: Science Press, 2003.
- [17] Petter Bjorstad, Mitchell Luskin. Parallel solution of partial differential equations[M]. New York: Springer-Verlag New York, 2000.